

Kick-off meeting,

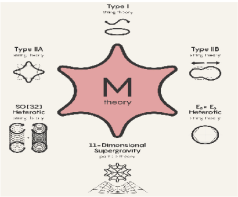
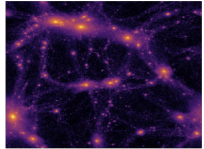
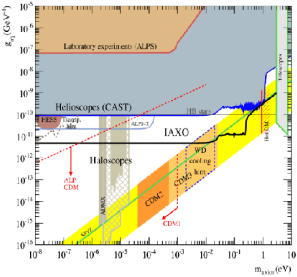
24th Feb. 2023

Axion-photon conversion in turbulent magnetic fields

Pierluca Carenza
OKC, Stockholm University

Motivations to study axions and ALPs

Axions and ALPs are a window on high-energy physics

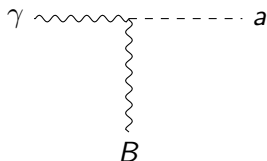


This hot topic is a motivation for interdisciplinary searches

ALP-photon oscillations

G. Raffelt and L. Stodolsky, Phys. Rev. D **37** (1988), 1237

Most of the phenomenology is related to ALP-photon conversions



Physics involved here:

- ▶ External magnetic field
- ▶ Axion mass and plasma frequency
- ▶ QED birefringence (high B)
- ▶ CMB refraction (high energy)

Axion detection

P. Sikivie, Phys. Rev. Lett. **51** (1983)

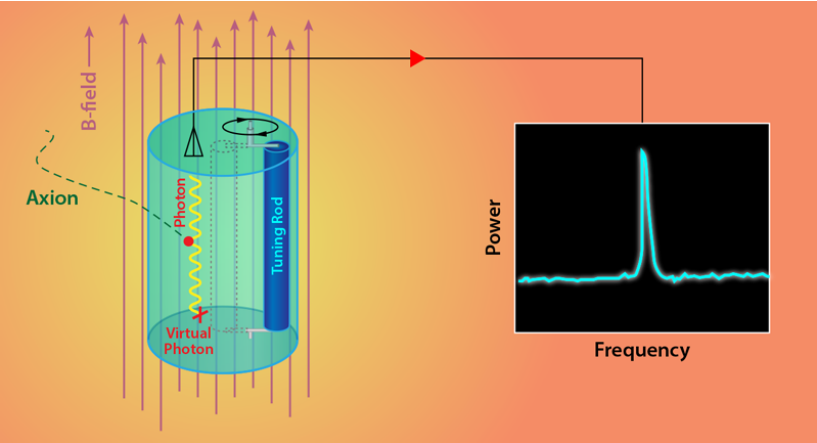
Axions can be detected by axion-photon conversion in an external magnetic field



- ▶ **Haloscopes:** DM axions
ADMX and MADMAX
- ▶ **Helioscopes:** solar axions
CAST and the future IAXO

Haloscopes

DM axions convert into photons in magnetic fields

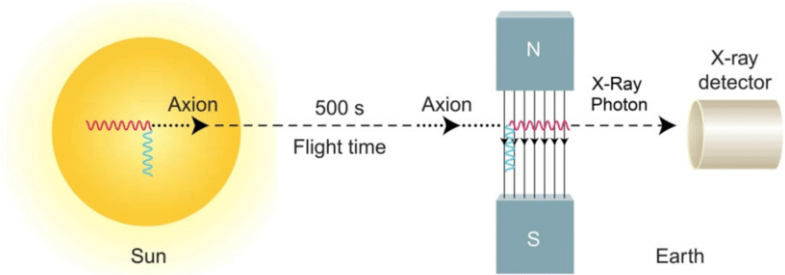


ADMX



Helioscopes

Axions are produced in the Sun via Primakoff effect in microscopic magnetic fields...



... and they convert into photons in macroscopic magnetic fields

CAST



Perturbative axion-photon conversion probability

M. C. D. Marsh, PC *et al.*, Phys. Rev. D **105** (2022) no.1, 016013

At the lowest order in $g_{a\gamma}$ the amplitude for the process is

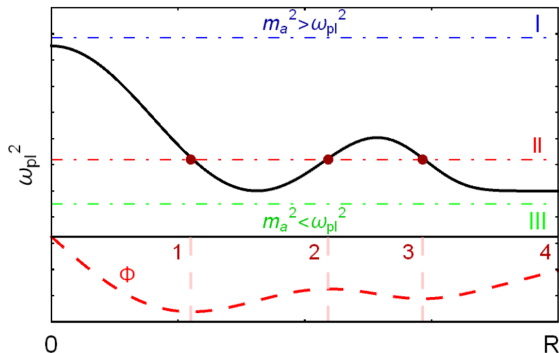
$$\mathcal{A}_{\gamma_i \rightarrow a} = -i \frac{g_{a\gamma}}{2} \int_{-\infty}^{\infty} d\rho u_{T,i} \cdot B(\rho u) e^{-i\Phi(\rho)}$$

where

$$\Phi(\rho) = \int_0^\rho d\rho' \frac{m_a^2 - \omega_{\text{pl}}^2}{2\omega}$$

where u is the photon propagation direction, $u_{T,i}$ indicate the photon polarization

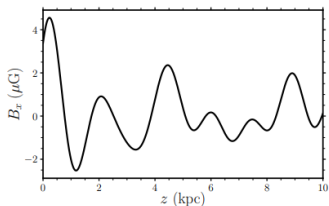
Which means...



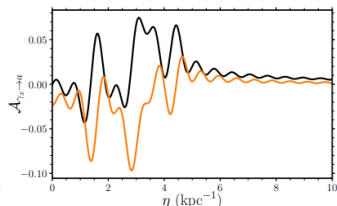
- ▶ Resonant conversions: $\Phi = 0$
- ▶ Massless axions: Fourier transform of B/ω_{pl}^2
- ▶ Massive axions: Fourier transform of B

Example in the massive case

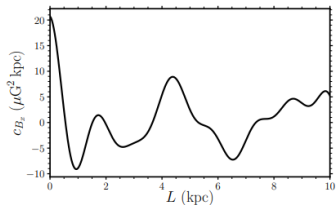
Spectral modulations are encoded in the power spectrum of B



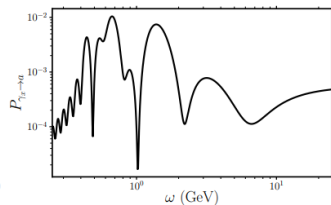
(a) Magnetic field profile.



(b) The real, $\text{Re}(\mathcal{A}_{\gamma_x \rightarrow a}) = \mathcal{F}_a(\Delta_x)$ (black), and imaginary, $\text{Im}(\mathcal{A}_{\gamma_x \rightarrow a}) = -\mathcal{F}_c(\Delta_x)$ (orange), parts of the amplitude $\mathcal{A}_{\gamma_x \rightarrow a}$.



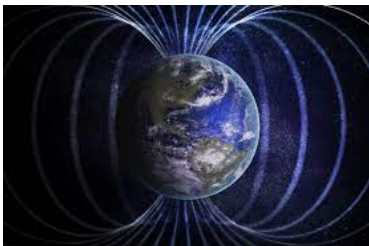
(c) Magnetic field autocorrelation function.



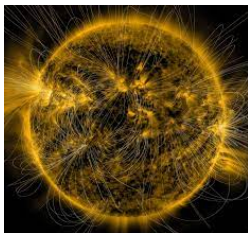
(d) Conversion probability as function of the axion energy.

Astrophysical magnetic fields: Earth and Sun

$B = 0.5 \text{ G}$ on the surface

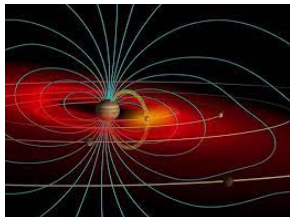


$B = 10 \text{ G}$ on the surface and $B = 2000 \text{ G}$ in sunspots



Astrophysical magnetic fields: Solar system and beyond

$B = 50 \mu\text{G}$ in the interplanetary space



$B = 1 - 5 \mu\text{G}$ in the Milky Way

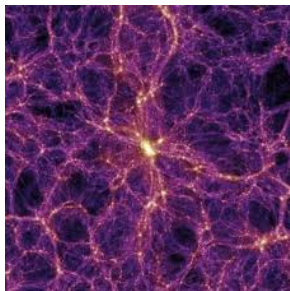


Astrophysical magnetic fields: two extremes

$B = 10^{12} - 10^{14}$ G in pulsars



$B = 10^{-9}$ G in the intergalactic space



Galaxy clusters

Hundreds of galaxies held together by gravity

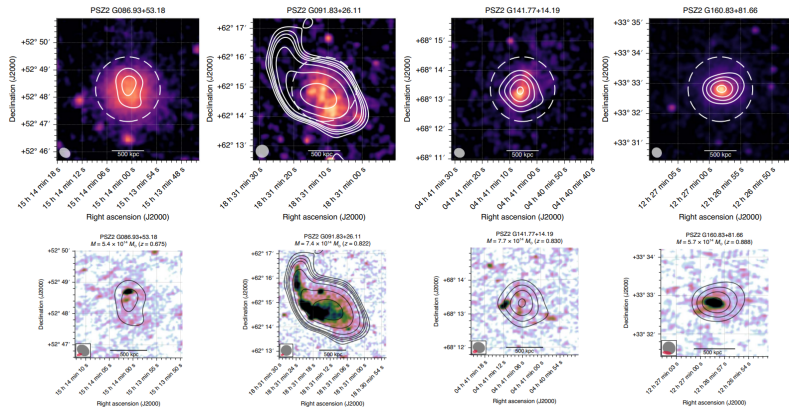


Among the largest structure in the Universe ($\sim 2 - 5$ Mpc)

Observations of GCs

Di Gennaro, G. *et al.*, Nat Astron 5, 268–275 (2021)

X-ray and radio are complementary probes



Galaxy cluster magnetic fields

F. Govoni and L. Feretti, Int. J. Mod. Phys. D **13** (2004), 1549-1594

The plasma in galaxy clusters is

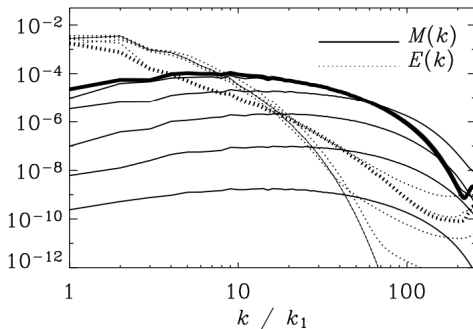
- ▶ Hot $\rightarrow T \sim 10$ keV
- ▶ Low-density $\rightarrow n_e \sim 10^{-3} \text{ cm}^{-3}$
- ▶ Magnetized $\rightarrow B \sim 10 \mu\text{G}$
- ▶ Coherent $\rightarrow l_{\text{coh}} \sim 10$ kpc

Galaxy clusters are huge axion detectors!!

Dynamo process

A. Brandenburg and K. Subramanian, Phys. Rept. **417** (2005), 1-209

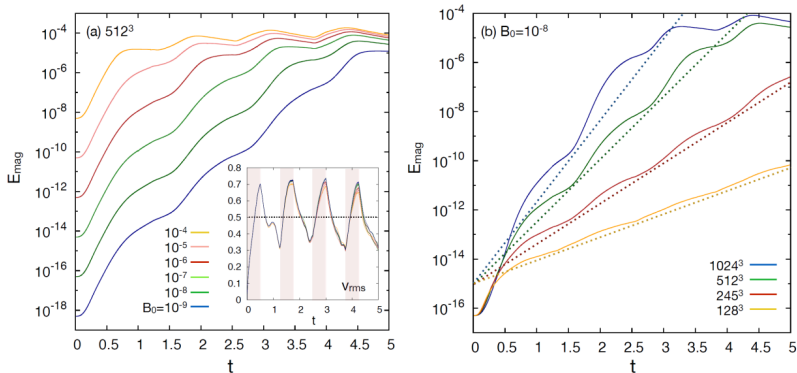
Kinetic energy is converted into magnetic energy



Exponential growth of the magnetic energy

S. Roh *et al.*, [arXiv:1906.12210 [astro-ph.HE]].

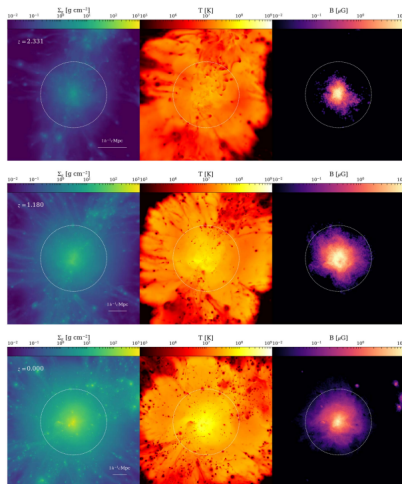
Dependence on initial seed (left) and exponential growth (right)



Simulated Galaxy Cluster

U. P. Steinwandel *et al.*, 2022 *ApJ* 933 131

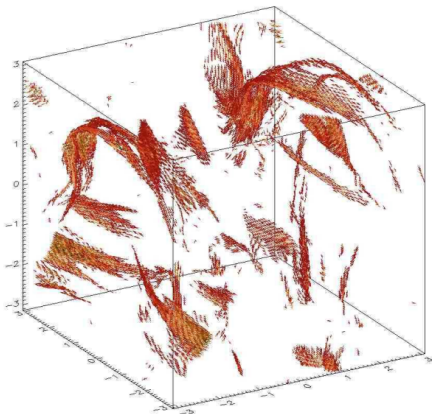
Density, temperature and magnetic field profile in high-resolution MHD simulations. Note the evolution after merging



Coherent structures

A. Brandenburg and K. Subramanian, Phys. Rept. **417** (2005), 1-209

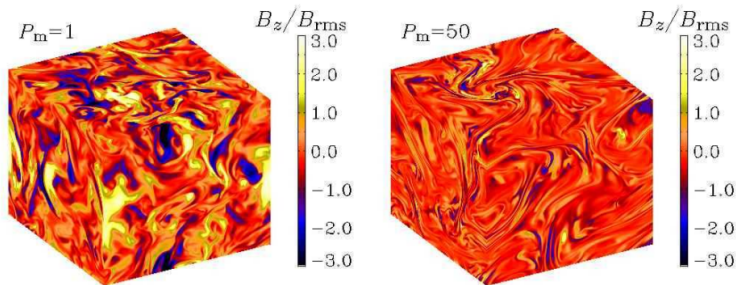
Large structures with $B > 4B_{\text{rms}}$, resistivity determines the thickness



Folded structures

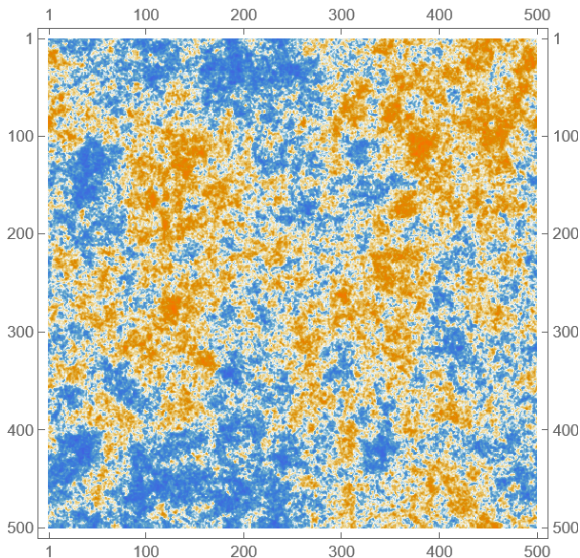
A. Brandenburg and K. Subramanian, Phys. Rept. **417** (2005), 1-209

Interesting B field have a large Prandtl number: momentum diffusivity \rightarrow ordered motion



Gaussian Random fields

Each $B_i(x, y, z)$ is a random variable with pdf $f_{B_i(x,y,z)}(b)$

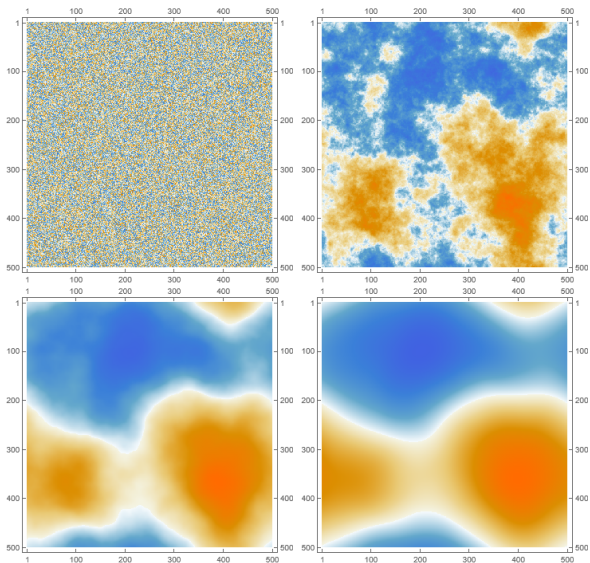


Generating a Random Field in 1D

- ▶ random white noise B_h
- ▶ Fourier transformed to \tilde{B}_h
- ▶ By construction $\langle \tilde{B}_h \tilde{B}_{h'} \rangle = \delta_{hh'}$
- ▶ Introduce non-gaussianities: $\tilde{B}_h \rightarrow f(\tilde{B}_h)$
- ▶ Redefine the field $\sqrt{P(k_h)} \tilde{B}_h$
- ▶ Back to the real space

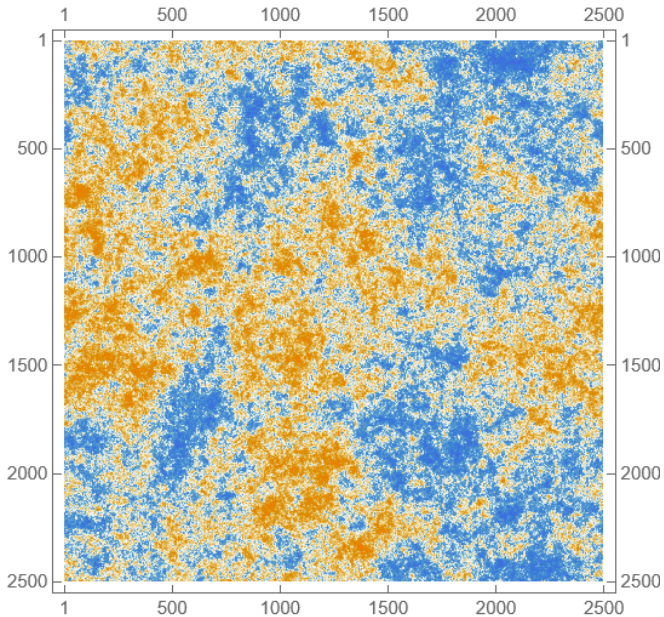
Power spectrum

The power spectrum is defined as $P(k) = \langle B(k)B^*(k) \rangle$



Plots for $P \sim k^{-n}$ with $n = 0, 3, 5, 7$

Scale invariance, $P \sim k^{-2}$

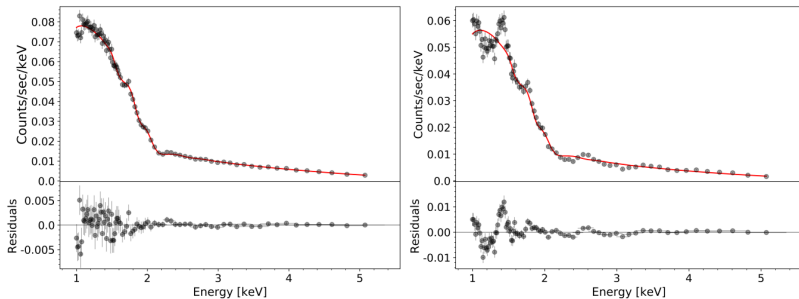


ALP bounds from Galaxy Clusters

S. Schallmoser *et al.*, [arXiv:2108.04827 [astro-ph.CO]].

Comparison: observed spectrum vs fake ALP signal

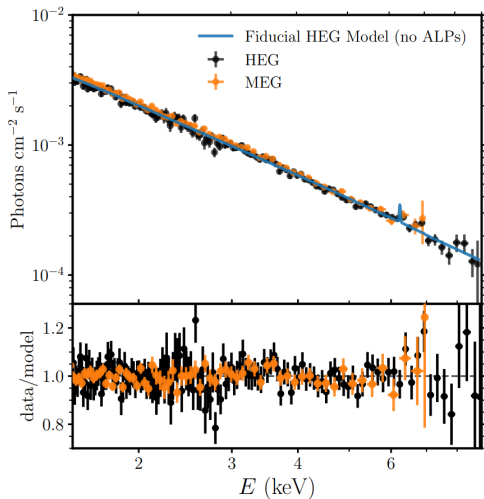
$$g_{a\gamma} = 5 \times 10^{-12} \text{ GeV}^{-1}$$



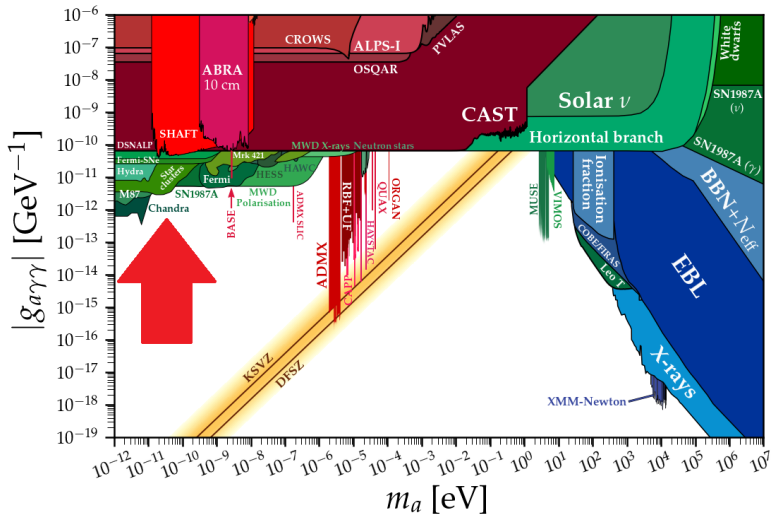
Constraint from NGC 1275

C. S. Reynolds *et al*, 2020 *ApJ* 890 59

The X-ray spectrum of NGC 1275 in the Perseus Cluster measured by Chandra might reveal axions



The strongest constraint for light axions

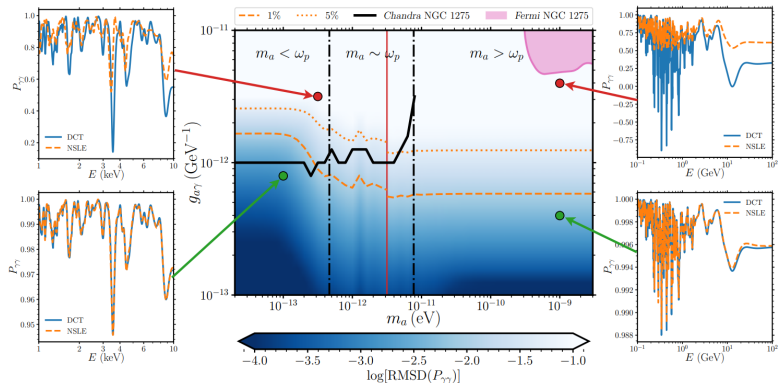


Questions about this constraint

- ▶ Future perspectives
- ▶ How to speed up the calculation?
- ▶ Robustness to variations of B

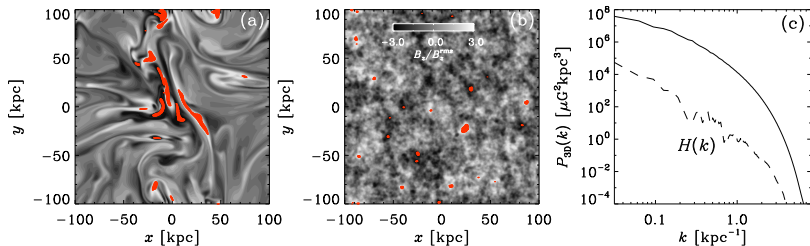
Applicability of the perturbative formulation

J. H. Matthews *et al.* *Astrophys. J.* **930** (2022) no.1, 90



MHD simulations vs GRF

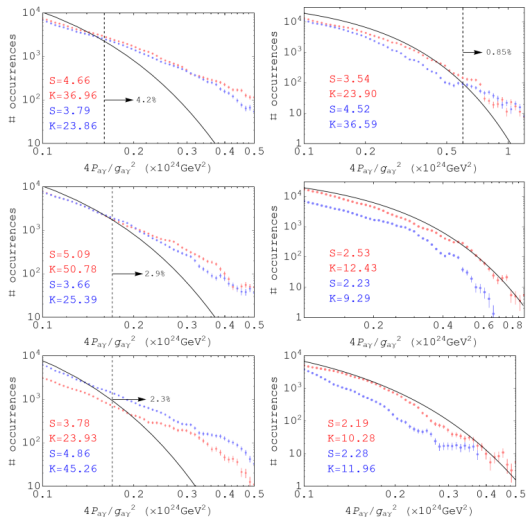
Same power spectrum but very different



Note the large structures and peaks

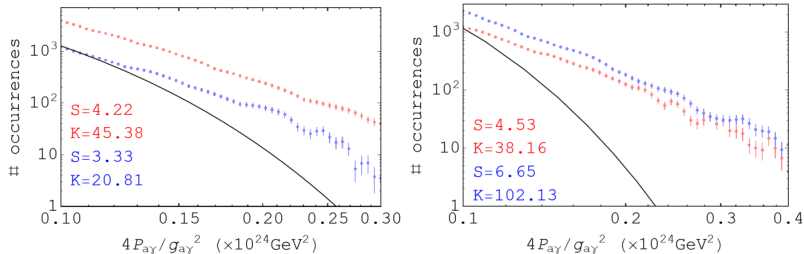
Differences in $P_{a\gamma}$: massive ALP case

PC, R. Sharma *et al.*, [arXiv:2208.04333 [hep-ph]].



Far from the Gaussian case $s = 2$ and $k = 9$

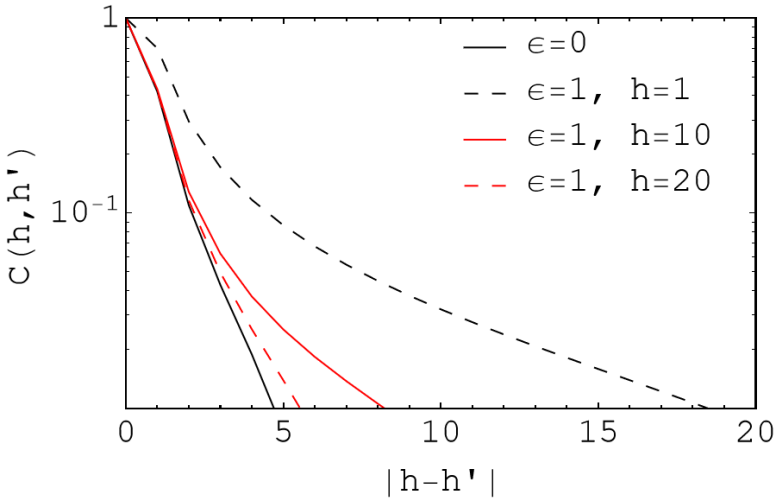
Differences in $P_{a\gamma}$: light ALP case



Same conclusions, more difficult for an analytical formulation. In the plot $m_a = 6.6 \times 10^{-12}$ eV and $\omega = 10$ keV.

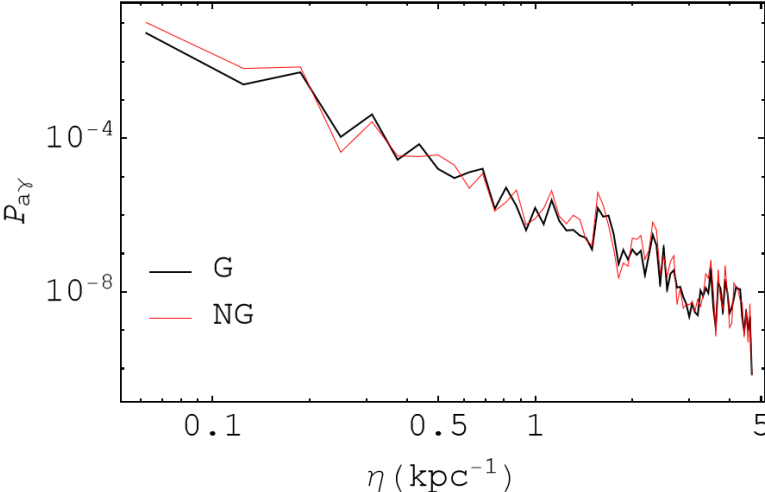
Effect of non Gaussianities: large coherent structures

The NG case shows coherent structures and more inhomogeneities



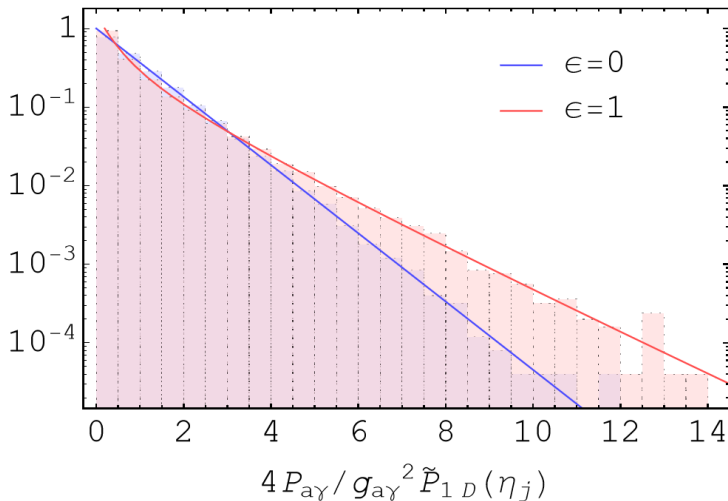
Effect of non Gaussianities: peaks of B

The NG case shows more evident peaks



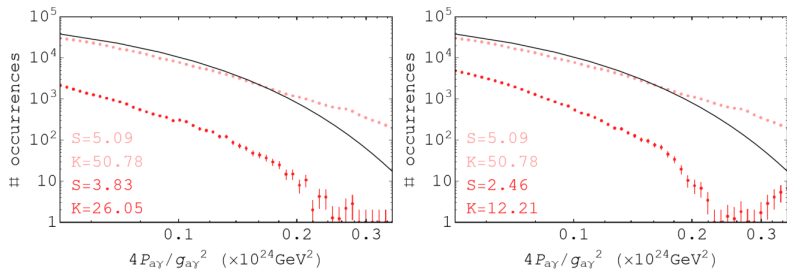
Heavy tails

In this toy model we reproduce a longer tail for the NG case



Responsible for the fat tails: non gaussianities

Masking coherent regions and peaks of B



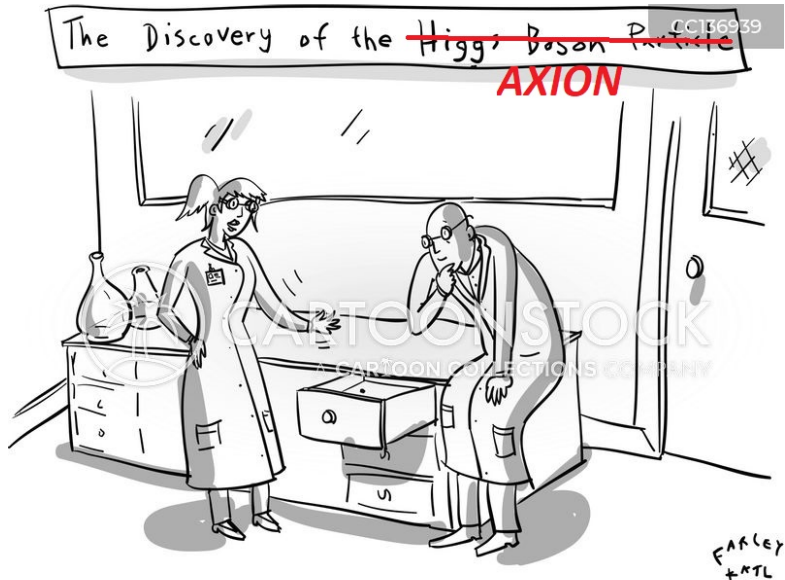
Going to the Gaussian case $s = 2$ and $k = 9$

Athena and axion signatures

The peculiar MHD features might be visible in high resolution experiments



Conclusions



"Always the last place you look!"